J Appl Physiol 112: 1393–1402, 2012.
First published January 12, 2012; doi:10.1152/japplphysiol.00511.2011.

Effect of development on $[Ca^{2+}]_i$ transients to ATP in petrosal ganglion neurons: a pharmacological approach using optical recording

Ana R. Nunes,[1,2] Raul Chavez-Valdez,[1,3] Tarrah Ezell,[1] David F. Donnelly,[4] Joel C. Glover,[5] and Estelle B. Gauda[1]

[1]*Pediatrics, Johns Hopkins Medical Institutions, Baltimore, Maryland;* [2]*CEDOC, Pharmacology, Faculdade de Ciências Medicas, Universidade Nova de Lisboa, Lisbon, Portugal;* [3]*Pediatrics, Texas Tech University-Health Sciences Center, Odessa, Texas;* [4]*Pediatrics, University School of Medicine, New Haven, Connecticut; and* [5]*Physiology, Institute of Basic Medical Sciences, University of Oslo, Oslo, Norway*

Submitted 26 April 2011; accepted in final form 5 January 2012

Nunes AR, Chavez-Valdez R, Ezell T, Donnelly DF, Glover JC, Gauda EB. Effect of development on $[Ca^{2+}]_i$ transients to ATP in petrosal ganglion neurons: a pharmacological approach using optical recording. *J Appl Physiol* 112: 1393–1402, 2012. First published January 12, 2012; doi:10.1152/japplphysiol.00511.2011.—ATP, acting through $P2X_2/P2X_3$ receptor-channel complexes, plays an important role in carotid body chemoexcitation in response to natural stimuli in the rat. Since the channels are permeable to calcium, P2X activation by ATP should induce changes in intracellular calcium ($[Ca^{2+}]_i$). Here, we describe a novel ex vivo approach using fluorescence $[Ca^{2+}]_i$ imaging that allows screening of retrogradely labeled chemoafferent neurons in the petrosal ganglion of the rat. ATP-induced $[Ca^{2+}]_i$ responses were characterized at postnatal days (P) 5–8 and P19–25. While all labeled cells showed a brisk increase in $[Ca^{2+}]_i$ in response to depolarization by high KCl (60 mM), only a subpopulation exhibited $[Ca^{2+}]_i$ responses to ATP. ATP (250–1,000 μM) elicited one of three temporal response patterns: fast (R1), slow (R2), and intermediate (R3). At P5–8, R2 predominated and its magnitude was attenuated 44% by the $P2X_1$ antagonist, NF449 (10 μM), and 95% by the $P2X_1/P2X_3/P2X_{2/3}$ antagonist, TNP-ATP (10 μM). At P19–25, R1 and R3 predominated and their magnitudes were attenuated 15% by NF449, 66% by TNP-ATP, and 100% by suramin (100 μM), a nonspecific P2 purinergic receptor antagonist. $P2X_1$ and $P2X_2$ protein levels in the petrosal ganglion decreased with development, while $P2X_3$ protein levels did not change significantly. We conclude that the profile of ATP-induced P2X-mediated $[Ca^{2+}]_i$ responses changes in the postnatal period, corresponding with changes in receptor isoform expression. We speculate that these changes may participate in the postnatal maturation of chemosensitivity.

peripheral arterial chemoreceptors; carotid body; petrosal ganglia neurons; P2X receptors; neurotransmitters; chemoexcitation

CHEMOSENSITIVE CELLS within the carotid body sense changes in the partial pressures of O_2 (Pa_{O_2}) and CO_2 (Pa_{CO_2}) in arterial blood and evoke increases in action potential activity in afferent nerve fibers that terminate in the brain stem. The essential neuronal structures that are involved in this response include the oxygen-sensing type 1 cells (glomus cells) in the carotid body and the chemosensory afferents whose cell bodies reside in the petrosal ganglion (Fig. 1). Hypoxia elicits type 1 cell depolarization, an increase of intracellular calcium ($[Ca^{2+}]_i$), and the release of neurotransmitters that can modulate, inhibit, or stimulate the afferent nerve fibers, thus changing the afferent neural drive to second-order neurons within the nucleus tractus solitarius (10, 12, 21).

At birth, the organ sensitivity to hypoxia is relatively low and increases to adult levels during the first 2–3 wk of postnatal life (13). In part, maturation is due to an increased responsiveness of type 1 cells, which show an increased depolarization and $[Ca^{2+}]_i$ response to hypoxia with age (36). In contrast, little is known about age-dependent changes of the afferent neurons, including their responsiveness to purported excitatory transmitters such as ATP. Although species differences have been reported, recent evidence in rodents strongly supports a major role for ATP, acting through $P2X_2/P2X_3$ receptors, in mediating hypoxic excitation of chemosensory afferents (1, 22, 24, 25, 33, 37). Afferent nerve activity is highly sensitive to P2X blocking agents and mice lacking $P2X_2/P2X_3$ receptors show greatly diminished ventilatory and chemoreceptor nerve activity responses to hypoxic challenge (25).

In this study we developed a novel ex vivo preparation to assay $[Ca^{2+}]_i$ responses to bath application of ATP in a subpopulation of chemoafferent cell bodies in the rat petrosal ganglia. By using different P2X receptor antagonists and observing the corresponding changes in the responses, we were able to better characterize the functional role of various P2X receptors during postnatal development. We found that the $[Ca^{2+}]_i$-response patterns of chemoafferents to ATP exhibit changes during postnatal development corresponding with changes in P2X receptor protein expression, indicating a change in purinergic receptor properties during the maturation of organ sensitivity.

MATERIALS AND METHODS

Animals. The Animal Care and Use Committee at the Johns Hopkins University School of Medicine approved all experimental protocols. We used male and female Sprague-Dawley rats (Charles River Laboratories, Wilmington, MA) between postnatal days (P) 5 and 8 (young group) and P19 and 25 (older group). All animals were briefly anesthetized with isoflurane (Abbott Laboratories, IL) and decapitated. We quickly removed en bloc the bifurcation of the carotid artery, including the carotid body (CB), the nodose/petrosal ganglion (NPG) complex, and the glossopharyngeal nerve. The CB and the NPG and intact neuronal connections were used for intracellular calcium imaging (CB/NPG complex). From another group of animals at the same postnatal ages, petrosal ganglia were microdissected from the nodose ganglia and processed for Western blotting, as outlined below.

Intracellular calcium imaging. The CB/NPG complex was incubated in trypsin (0.02%; Sigma, St Louis, MO) and collagenase (0.01%, Sigma) at 37°C to aid in removal of connective tissue and

Address for reprint requests and other correspondence: E. B. Gauda, Dept. of Pediatrics, Division of Neonatology, Johns Hopkins Medical Institutions, 600 N. Wolfe St., CMSC 6-104, Baltimore, MD 21287-3200 (e-mail: egauda@jhmi.edu).

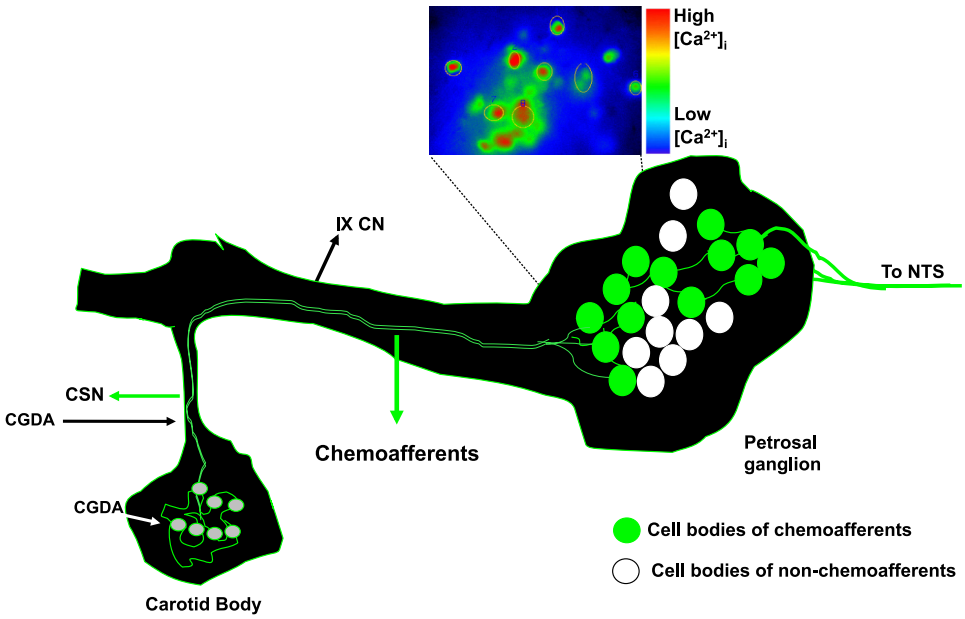

Fig. 1. Schematic diagram illustrating the sites of calcium green dextran amine application (CGDA) and respective identification of the retrogradely labeled petrosal ganglia neurons (PGNs, green cell bodies), with representative video image showing the intracellular Ca^{2+} concentration ($[Ca^{2+}]_i$) responses in the region of interest (40×, color-coded, with the red end of the spectrum representing highest intensity). CSN, carotid sinus nerve; IX CN, 9th cranial nerve; NTS, nucleus tractus solitarius.

increase the permeability to exogenous drugs. Because connective tissue increased with age, incubation time in trypsin/collagenase was 5 min for tissues removed from the younger animals and up to 30 min for tissues removed from the older animals. The CB/NPG complex was then placed in ice-cold 60% O_2-5% CO_2 equilibrated Ringer's solution containing (in mM) 125 NaCl, 5 KCl, 1 NaH_2PO_4, 1 $MgCl_2$, 11 glucose, 26 $NaHCO_3$, 2 $CaCl_2$, pH 7.4. Retrograde labeling of chemoreceptor afferent neurons with calcium green-1 dextran-amine (CGDA, 3 kDa, Molecular Probes, Eugene, OR) from the CB was performed in preparations from young (n = 4) and older (n =8) groups of animals, as previously described with minor modifications (9, 31). In brief, CGDA was dissolved to saturation in PBS (1 μl of 1 M, Quality Biological) containing brain-derived neurotrophic factor (BNDF, 5 ng/ml, Sigma) and glial cell-derived neurotrophic factor (GDNF, 5 ng/ml, Sigma). The dye in solution was dried into a crystal on the tip of a stainless steel insect pin that had been glued to the end of a glass pipette. Three crystals were placed on the CB previously fenestrated with a 2-μm tip diameter glass microelectrode. Excess dye was rapidly removed using a suction catheter. In a few preparations the CGDA crystals were applied to the freshly cut end of the carotid sinus nerve (n = 6 per group). After labeling, we incubated the CB/NPG complex overnight in Ringer's solution equilibrated with 60% O_2-5% CO_2-35% N_2, pH 7.4, at room temperature. On the following day, the CB/NPG complex was transferred into a heated chamber (Warner Instruments, Hamden, CT) and superfused with Ringer's solution equilibrated with 60% O_2-5% CO_2-35% N_2 at 32°C using a perfusion pump (Ismatec, Cole Parmer Instrument, Vernon Hills) at constant flow rate of 4 ml/min.

The CGDA-labeled cell bodies of chemoafferents within the petrosal ganglia (Fig. 1) were visualized with a 40× water immersion objective using a Nikon Eclipse Fluorescent E-400 microscope (Nikon Instruments, Melville, NY) with a FITC filter (abs/em 494/519). Regions containing individual CGDA-labeled cells were selected and identified as regions of interest. Fluorescence images were acquired with a CCD camera (Hamamatsu, Photonic Systems, Bridgewater, NJ). To minimize photobleaching during the recordings, the illumination, controlled by X-cite-Series 1200 PC illuminator (Exfo Photonic Solutions, Ontario, Canada), was set at the lowest intensity and additional neutral density filters were used. The same filter settings were used throughout the experiment and photobleaching was negligible (0.67 ± 0.46% change between baseline level at the beginning vs. at the end of the recording). Changes in fluorescence (ΔF) were measured using iVision (BioVision Technologies, Exton, PA) and expressed as a ratio of change in fluorescence to baseline fluorescence × 100 (ΔF/F, see *Data analysis* below). Cells with a relative change in fluorescence intensity (ΔF/F) ≥ 2% were considered responsive. Viability of the cells was assessed by a 30-s exposure to depolarizing Ringer's solution with high KCl concentration (in mM: 70 NaCl, 60 KCl, 1 NaH_2PO_4, 1 $MgCl_2$, 11 glucose, 26 $NaHCO_3$, 2 $CaCl_2$, pH 7.4). Those cells responding to the KCl stimulus were further tested to determine their response to increasing ATP concentrations (250–1,000 μM, Sigma). In a subset of experiments, after exposure to ATP, we subsequently incubated the CB/NPG complex with P2XR antagonists: suramin (100 μM, nonspecific P2 purinergic receptor antagonist, Sigma), TNP-ATP (10 μM, $P2X_1$/$P2X_3$/$P2X_{2/3}$ antagonist, Sigma), or NF449 (10 μM, $P2X_1$ antagonist, Tocris Bioscience, Ellisville, MO) in Ringer's solution for 30 min. Then we applied ATP in the presence of P2XR antagonist for 30 s and recorded changes in fluorescent intensity during 160 s, followed by a 45-min washout period with normal Ringer's solution. We assessed recovery and reproducibility of the calcium response recovery by reexposing the preparation to the same concentration of ATP. At the end of each experiment we applied Ringer's KCl 60 mM to check for cellular viability. To study the contribution of *1*) extracellular calcium, *2*) voltage-gated calcium channels, and *3*) intracellular calcium store $[Ca^{2+}]_i$ on changes in $[Ca^{2+}]_i$ responses to ATP (1,000 μM) and KCl (60 mM), we incubated the preparation in Ca^{2+}-free Ringer's with EGTA (1 mM, to remove extracellular calcium), nifedipine (50 μM, an L-type voltage-sensitive calcium channel blocker), ω-conotoxin (1 μM, an N-type voltage-sensitive calcium channel blocker), and ryanodine (10 μM, a blocker of Ca^{2+} release from intracellular stores), respectively.

ATP, P2XR antagonists, and ω-conotoxin were dissolved in distilled H_2O to a stock concentration of 0.1 M of ATP, 0.01 M of suramin, 0.0063 M of TNP-ATP, 1 mM of NF449, and 330 μM of ω-conotoxin. Nifedipine was dissolved in DMSO to a stock concentration of 0.010 M and ryanodine was dissolved in ethanol to a stock concentration of 0.010 M. The final concentration of DMSO and ethanol in the bath solution was 0.1% (vol/vol). The stock solutions were quickly frozen and stored at −20°C. Aliquots of ATP and antagonists were thawed and diluted to the appropriate concentrations in Ringer's solution just prior to use in the experiments.

Protein expression using Western blot. Petrosal ganglia were dissected free by excising the region where the glossopharyngeal nerve

joins the nodose ganglion; this is the region that contained the majority of the retrogradely labeled cell bodies in the calcium imaging experiments. Petrosal ganglia were quick-frozen and homogenized in buffer containing 20 mM Tris HCl, 1 mM EDTA, 5 mM EGTA, 10 mM benzamidine, 0.1 mM phenylmethylsulfonyl fluoride (all from Sigma), protease inhibitor cocktail (Complete, Roche Diagnostics, Indianapolis, IN), and 10% sucrose. Protein concentration was determined using the Bradford method (3) modified for microplate protein assay (Bio-Rad protein assay kit, Bio-Rad laboratories, Hercules, CA). Approximately 30 μg of homogenized protein was separated using a 15% SDS-PAGE. The protein was transferred to a nitrocellulose membrane, blocked with 5% nonfat dry milk and 0.1% Tween 20 in 1× Tris buffered saline (TBS, 20 mM Tris, 500 mM NaCl, pH 7.5, Bio-Rad) for 1 h. Primary antibodies were rabbit polyclonal anti-$P2X_1$ (1:500, sc-25692, Santa Cruz Biotechnology, Santa Cruz, CA), rabbit polyclonal anti-$P2X_2$ (1:500, sc-25693, Santa Cruz Biotechnology), rabbit polyclonal anti-$P2X_3$ (1:500, sc-25694, Santa Cruz Biotechnology), and monoclonal mouse anti-β-actin antibody (1:40,000, A2228, Sigma) as a protein loading control. After overnight exposure to each primary antibody, membranes were washed with 5% nonfat dry milk and 0.1% Tween-20 in TBS and exposed to goat anti-rabbit or anti-mouse secondary antibody (1:20,000, Bio-Rad) for 1 h. Membranes were developed with enhanced chemiluminescence using SuperSignal kit (Thermo Scientific, Rockford, IL), stripped for 30 min with Review Western Blotting stripping buffer solution (BioExpress, Kaysville, UT), and reincubated with primary antibody. Protein levels are reported as optical density (OD) and corrected for loading control.

Data analysis. Changes in fluorescence intensity from individual cells within a region of interest, reflecting $[Ca^{2+}]_i$ responses, were expressed as percent change in fluorescence intensity ($\Delta F/F \times 100$) as described above. Baseline levels were obtained by averaging the fluorescent signal obtained during 20 s prior to the drug challenge. Only the PGNs with a mean fluorescence response over 2% were considered for analysis. Responses were characterized by magnitude (area under the curve), rise time (time to peak), decay time, and peak amplitude. The magnitude of the response was quantified using GraphPad Prism (GraphPad Software, version 5, San Diego, CA) as the area under the ΔF/F above baseline vs. time graph, and, as such, has units of seconds (i.e., ΔF/F is unitless, and time was measured in s). Rise time was calculated by measuring the time of onset of the rise in fluorescence intensity to the time it reached peak intensity. Decay time was calculated by measuring the time required to reach the fluorescence baseline after the peak. Peak amplitude was measured as ΔF/F (%). Onset latency was not used as an experimental parameter because time of drug application was not consistently captured on line.

Statistical analysis. All data are presented as means ± SE, and *n* indicates either number of cells tested or preparations used, for intracellular calcium experiments, or *n* indicates number of litters for Western blot. Two-way repeated-measures ANOVA with Bonferroni's comparison test (GraphPad Prism) was used to determine differences between young and older groups in the change in fluorescent intensity from baseline. Age was a grouping variable and different dosages of ATP were used for repeated measures. Unpaired *t*-test was used to determine differences in magnitude of the response mediated by KCl between groups, and to determine changes in protein expression between young and older animals. Paired *t*-test was used to determine changes in the ATP-induced $[Ca^{2+}]_i$ responses in the absence and presence of selective and nonselective P2X antagonists. Last, Yates' chi-square and Cochran's *Q*-test were used to determine the difference in the percentages of responsive cells at the different dosages of ATP between young and older animals (IBM SPSS18, IBM Corporation, Armonk, NY). Significance was considered at the level of $P < 0.05$.

RESULTS

Identification of retrogradely labeled petrosal ganglion neurons (PGNs). Application of CGDA to the carotid body or to the carotid sinus nerve retrogradely labeled chemosensory afferent cell bodies in the petrosal ganglia (Fig. 1). The distal portion of the petrosal ganglia, which contains the chemosensory neurons (8), contained a similar number of retrogradely labeled neurons in younger and older animals whether the tracer application was in the carotid body (20.1 ± 2.5, $n = 9$ vs. 18.5 ± 2.2, $n = 8$, respectively; $P = 0.6$ unpaired *t*-test) or at the bifurcation of the carotid sinus nerve (21.3 ± 2.8, $n = 6$ vs. 21.6 ± 3.8, $n = 5$, respectively; $P = 1.0$).

To assess the viability of retrogradely labeled neurons, we applied a 30-s stimulus of high KCl (60 mM) to each preparation and monitored for changes in fluorescence intensity. High KCl induced a robust $[Ca^{2+}]_i$ response, presumably through depolarization and activation of voltage-gated calcium channels (Fig. 2). Only those preparations that exhibited KCl-induced $[Ca^{2+}]_i$ responses were further stimulated with ATP in the presence or absence of P2XR antagonists. Representative photomicrographs showing changes in fluorescence intensity in response to KCl (60 mM) in labeled PGN from animals at P7 and P25 are shown in Fig. 2, *A* and *B*. The magnitude of the $[Ca^{2+}]_i$ response to KCl in preparations from younger and older animals was 1,854 ± 206 ($n = 12$) and 1,766 ± 296 units ($n = 11$), respectively ($P = 0.8$).

ATP activates a subpopulation of PGNs in both younger and older animals. Bath application of ATP (250–1,000 μM) induced $[Ca^{2+}]_i$ responses in a subset of the CGDA-labeled PGNs that responded to high KCl. The number of total responsive PGNs was greater with increasing concentrations of ATP, and similar between younger and older animals [$P < 0.001$, ATP 250 vs. 500 vs. 1,000 μM, younger ($n = 300$) or older ($n = 309$), Cochran's *Q*-Test, Table 1]. Increasing ATP concentration increased the magnitude (area under the curve) and peak amplitude of the responses as shown by representative waveforms from the same PGN stimulated with ATP 250 μM (Fig. 3*A*), 500 μM (Fig. 3*B*), and 1,000 μM (Fig. 3*C*). Increasing ATP concentration from 250 to 1,000 μM increased peak amplitudes ($P < 0.001$) and magnitudes ($P < 0.001$) of responsive cells equally between both groups of animals (Fig. 3, *D* and *E*).

Developmental changes in ATP-induced $[Ca^{2+}]_i$-response patterns in PGNs. Whereas the number of ATP-responsive PGNs did not differ between the two age groups, the $[Ca^{2+}]_i$-response patterns of the PGNs did. The rise and decay of $[Ca^{2+}]_i$ responses induced by ATP in PGNs followed three distinct profiles (R1, R2, and R3, Fig. 4). R1 had a fast rise (time to peak, 13.2 ± 2.9 s) with a fast early decay (9.0 ± 0.8 s) followed by a slower late decay (88.6 ± 4.9 s, $n = 39$). R2 had a slow rise (time to peak, 33.4 ± 0.7 s) and a slow decay (77.0 ± 1.7 s, $n = 228$). R3 had a moderately fast rise (time to peak, 21.01 ± 1.1 s) but the slowest decay (90.9 ± 2.8 s, $n = 106$). Although the three response patterns were observed in both age groups for all concentrations of ATP (250–1,000 μM), R2 was more frequent in P5–8 animals, whereas R1 and R3 were more frequent in P19–25 animals ($P < 0.001$; χ^2 test; Table 1). The predominance of R2 persisted in the younger animals even at the higher doses of ATP (Table 1).

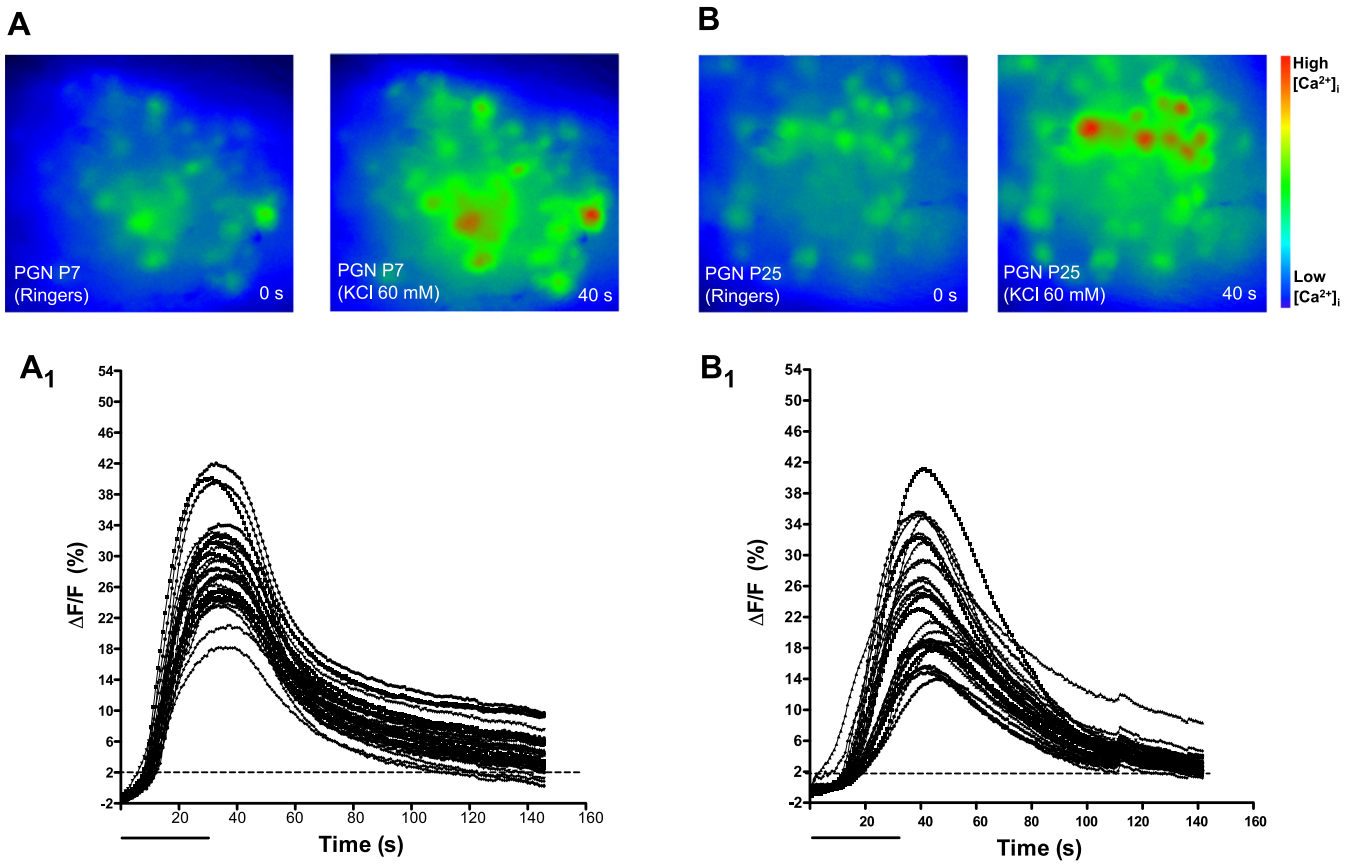

Fig. 2. Cell bodies of retrogradely petrosal ganglia neurons (PGN) exhibiting [Ca^{2+}]$_i$ responses to KCl (60 mM). Representative video images of retrogradely labeled PGNs showing fluorescence intensity (color coded, with the red end of the spectrum representing highest intensity) prior to (0 s) and at the peak of [Ca^{2+}]$_i$ response to KCl (40 s) in preparations from younger [postnatal day (P) 7; *A*] and older animals (P25; *B*). Representative tracings showing the percent change in mean fluorescence intensity (ΔF/F%) reflecting [Ca^{2+}]$_i$ response to KCl: younger (P7; A_1) and older animals (P25; B_1). Each line in the traces represents a single cell response. Horizontal bar indicates the duration of KCl exposure in the bath (30 s). Dashed line corresponds to 2%, arbitrarily defined as the response detection threshold.

Effect of P2XR antagonists on the ATP-induced responses of PGNs. To determine if the ATP-induced responses of PGNs were mediated by different P2XR subunits, we bath applied nonspecific and specific P2XR antagonists from 30 min prior to and throughout exposure to ATP.

Suramin, a nonselective P2 purinergic receptor antagonist that blocks $P2X_1$, $P2X_2$, $P2X_3$, $P2X_5$, and $P2X_7$ and P2Y receptors (23), essentially blocked all [Ca^{2+}]$_i$ responses in older animals, decreasing peak amplitude by 93.6 ± 2.0% ($P < 0.01$, $n = 10$, paired *t*-test) and magnitude by 99.9 ± 0.04 % ($P < 0.01$, $n = 10$, paired *t*-test, see Fig. 6), for all response types averaged together. After washout of suramin, KCl (60 mM) induced a [Ca^{2+}]$_i$ response in all the PGNs, with an identical magnitude as seen prior to the blockade ($P = 0.7$, $n = 24$), confirming the subsequent viability of the cells.

Suramin is known to modulate the activity of ryanodine receptors (RyR) (26). Since recorded [Ca^{2+}]$_i$ responses could be due to either entry of extracellular calcium through P2XRs (and possibly other calcium channels that open as a result of depolarization) or release from intracellular stores

Table 1. *Characterization of the [Ca^{2+}]$_i$-response profile in petrosal ganglia neurons to different concentrations of ATP (250–1,000 μM)*

ATP (μM):	250[a]		500[b]		1,000[b]	
Age Group:	P5-8	P19-25	P5-8	P19-25	P5-8	P19-25
			Response			
PGN[e]	7.4% (23/309)	9.7% (28/300)	26.0%[d] 80/309	21% (55/300)	31.4% (97/309)	39% (107/300)
RP1 PGN	0% (0/23)	25% (7/28)	2.5% (2/80)	20% (11/55)	5.2% (5/97)	12% (13/107)
RP2 PGN[c]	95.7% (22/23)	50% (14/28)	83.8% (67/80)	25.5% (14/55)	77.3% (75/97)	47% (50/107)
RP3 PGN	4.3% (1/23)	25% (7/28)	13.8% (11/80)	54.5% (30/55)	17.6% (17/97)	41% (44/107)

RP, response profile; PGN, petrosal ganglia neurons; P, postnatal day. [a]$P < 0.01$ (RP, P5–8 vs. P19–25); [b]$P < 0.001$ (RP, P5–8 vs. P19–25), [c]$P < 0.001$ (RP2 vs. RP1 or RP3, P5–8 vs. P19–25), [d]$P < 0.05$ (vs. P19–25). Yates' chi-square used in all cases. [e]$P < 0.001$ (ATP 250 vs. 500 vs. 1,000 μM, P5–8 or P19–25, Cochran's *Q*-test).

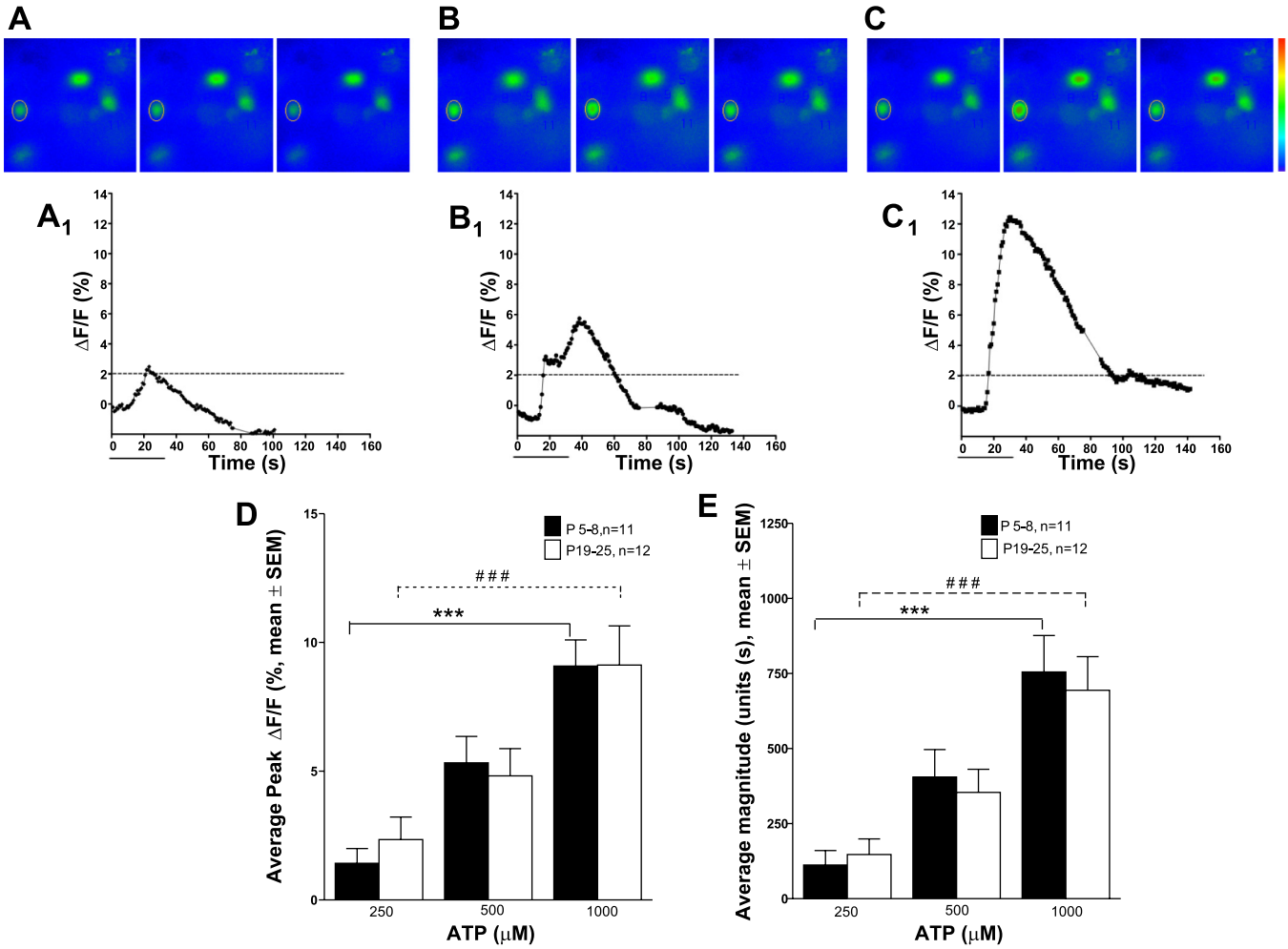

Fig. 3. [Ca^{2+}]$_i$ responses to different concentrations of exogenous ATP (250–1000 μM). Representative video images of a PGN from a P19–25 group exposed to ATP [250 (*A*), 500 (*B*) and 1,000 (*C*) μM] and corresponding response R3 waveforms (A_1, B_1, and C_1). Higher concentrations of ATP increased the mean response [measured as fluorescence intensity relative to baseline (ΔF/F) × 100]. The mean peak amplitude (*D*) and mean magnitude (*E*) of the [Ca^{2+}]$_i$ responses to different concentrations of ATP (250–1,000 μM). Increasing concentrations of ATP increased peak amplitude and magnitude of the [Ca^{2+}]$_i$-responses in both age groups: ***$P < 0.001$ in P5–8 group and ###$P < 0.001$ in P19–25 group; repeated-measures ANOVA; *n*, number of preparations.

(for example by the activation of RyRs), interpretation of the suramin blockade was ambiguous. We therefore turned to more specific PX2R blockers to identify the source for the calcium increase.

We first assessed the effects of TNP-ATP (10 μM), an antagonist of P2X$_1$, P2X$_3$, and heterodimeric P2X$_{2/3}$ receptors (34), and NF449 (10 μM), a specific P2X$_1$ antagonist, on the average peak amplitudes and magnitudes of the response in younger and older animals, independent of response type. In younger animals, peak amplitudes and magnitudes were decreased by about 90% by TNP-ATP ($n = 35$) and by about 40% and 50%, respectively, by NF449 ($n = 12$). In older animals, the same antagonists were less effective. Peak amplitudes and magnitudes were decreased by about 60% by TNP-ATP ($n = 35$) and by about 20% and 30%, respectively, by NF449 ($n = 12$). Therefore, we conclude that in younger animals about half of the response is mediated by P2X$_1$ and most of the remainder is mediated by some combination of P2X$_3$ and heterodimeric P2X$_{2/3}$, whereas in older animals about a third to half of the response is mediated by P2X$_1$, a small proportion is mediated by some combination of P2X$_3$ and heterodimeric P2X$_{2/3}$, and 40% is mediated by other purinergic receptors.

The antagonists did not affect the different response types equally. In younger animals, in which R1 was infrequently observed, TNP-ATP and NF449 decreased R2 magnitude by about 95% and 50%, respectively, and R3 magnitude by about 80% and 40%, respectively (Fig. 5, Fig. 6, A_1–A_4, and Fig. 7, A_1–A_4). In older animals, TNP-ATP and NF449 decreased R1 magnitude by about 5% each; R2 magnitude by about 75% and 25%, respectively; and R3 magnitude by 75% and by almost nothing, respectively (Fig. 5, Fig. 6, B_1–B_4, and Fig. 7, B_1–B_4). We conclude that R1 is mediated primarily by purinergic receptors other than P2X$_1$, P2X$_3$, and P2X$_{2/3}$, that R2 has a P2X$_1$-mediated component and a P2X$_3$- and/or P2X$_{2/3}$-mediated component that diminishes with development, and that R3 has practically no P2X$_1$-mediated component and a P2X$_3$- and/or P2X$_{2/3}$-mediated component that is relatively stable with development. R2 and R3 each have a minor component mediated by purinergic receptors other than P2X$_1$, P2X$_3$, and P2X$_{2/3}$ that increases with development.

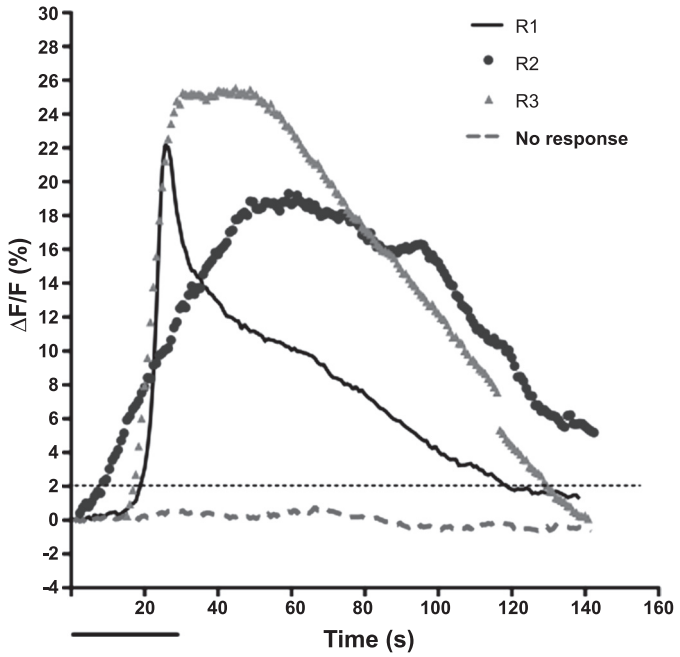

Fig. 4. Three different response waveforms generated by changes in $[Ca^{2+}]_i$ responses to ATP observed in a subpopulation of PGNs. R1 (solid black line) shows a rapid rise with sustained decay, R2 (circle) shows a slow rise with a slow decay, and R3 (triangle) shows a fast rise but slow decay. The dashed gray line depicts cells with no change in $[Ca^{2+}]_i$ responses to ATP. Horizontal bar indicates the duration of the ATP application (30 s).

Contribution of voltage-gated calcium channels on the ATP-induced responses of PGNs. We studied the contribution of extracellular calcium on high KCl and ATP response. For those experiments, we incubated the preparation in Ca^{2+}-free Ringer's in the presence of EGTA (1 mM). After 10 min of incubation, a stimulus of ATP (1,000 μM, 30 s) or KCl (60 mM, 30 s) did not induce an increase in intracellular calcium (n = 11 PGNs). Further incubation in Ca^{2+}- containing Ringer's for 10 min completely reversed the response to ATP and high KCl. These results suggested that Ca^{2+} responses to ATP and high KCl depended on extracellular calcium.

To test the contribution of the voltage-gated calcium channels to the increase in intracellular calcium levels, we studied the effect of nifedipine (50 μM, an L-type voltage-sensitive calcium channel blocker) and ω-conotoxin (1 μM, an N-type voltage-sensitive calcium channel blocker) in the presence of ATP (1,000 μM) or high KCl (60 mM). Preincubation with nifedipine (50 μM) for 40 min decreased KCl response by 63.7 ± 6.2% (n = 26) and ATP response by 50.2 ± 10.5% (n = 26). Nifedipine plus ω-conotoxin (1 μM) applied for 20 min blocked the KCl response by 93.0 ± 1.8% (n = 13) and partially decreased the ATP response by 52.6 ± 12.4% (n = 13). In the presence of a cocktail of ryanodine (10 μM), a potent inhibitor of Ca^{2+} release from intracellular stores, nifedipine and ω-conotoxin ATP responses were blocked by 82.3 ± 5.2% (n = 3). The inhibitory effects of these blockers were reversed following a 40-min washout of the drugs or replacement of extracellular calcium. These results suggest *1*) extracellular calcium that enters the cell through P2X receptors, *2*) voltage-gated calcium channels, and *3*) calcium release from intracellular sources all contribute to the increase in intracellular calcium PGNs in response to ATP.

Developmental changes in the P2XR protein expression profile in PGNs. Based on our pharmacological experiments, we deduced that some combination of $P2X_1$, P2X3, and the heteromeric receptor $P2X_{2/3}$ mediates virtually all of R2 and most of R3 in younger animals, substantially less of R2 and R3 in older animals, but very little of R1. To determine whether developmental changes in P2XR subtype protein levels in PGNs might account for these different pharmacological response profiles, we assessed protein levels by Western blot. With development from younger to older ages, $P2X_1$ and $P2X_2$ protein levels decreased by 60% ($P < 0.05$, n = 5) and 67% ($P < 0.05$, n = 5), respectively, while $P2X_3$ levels did not change ($P > 0.05$, n = 5) (Fig. 8). Thus, the profile of P2XR protein changes with development in a way that is consistent with the changes in pharmacological sensitivity.

DISCUSSION

In this study, using a novel ex vivo preparation of the petrosal ganglion in which chemoreceptor neurons are retrogradely labeled with the calcium sensitive tracer CGDA, we investigated the differences between younger (P5–8) and older (P17–25) animals in *1*) $[Ca^{2+}]_i$-response patterns to different concentrations of ATP during pharmacological blockade of P2XRs, and *2*) differences in P2XR-isoform protein levels in

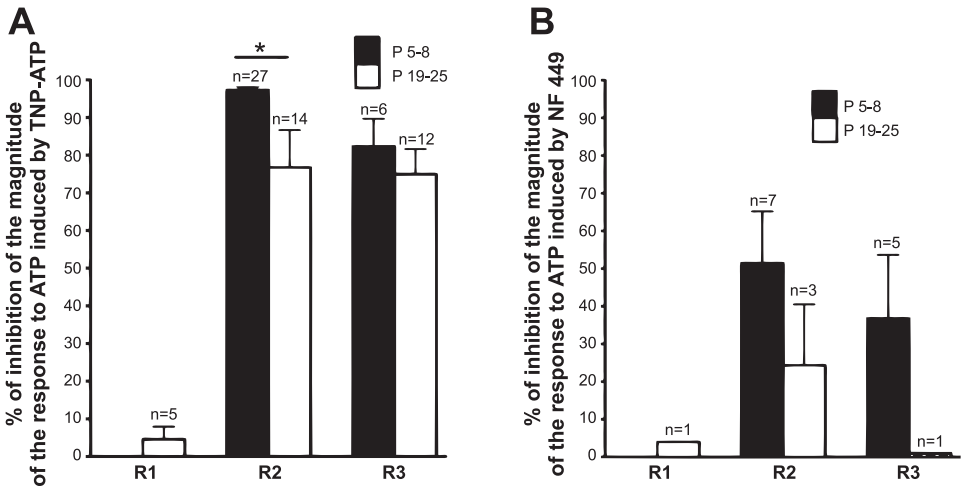

Fig. 5. Effect of P2X receptor antagonists TNP-ATP (10 μM; *A*) and NF449 (10 μM; *B*) on the magnitude (area under the curve) of the $[Ca^{2+}]_i$ responses (R1, R2, and R3) to ATP in PGNs from P5–8 group and P19–25 group of animals. *$P < 0.05$ between age groups, paired t-test. n, number of petrosal ganglia neurons.

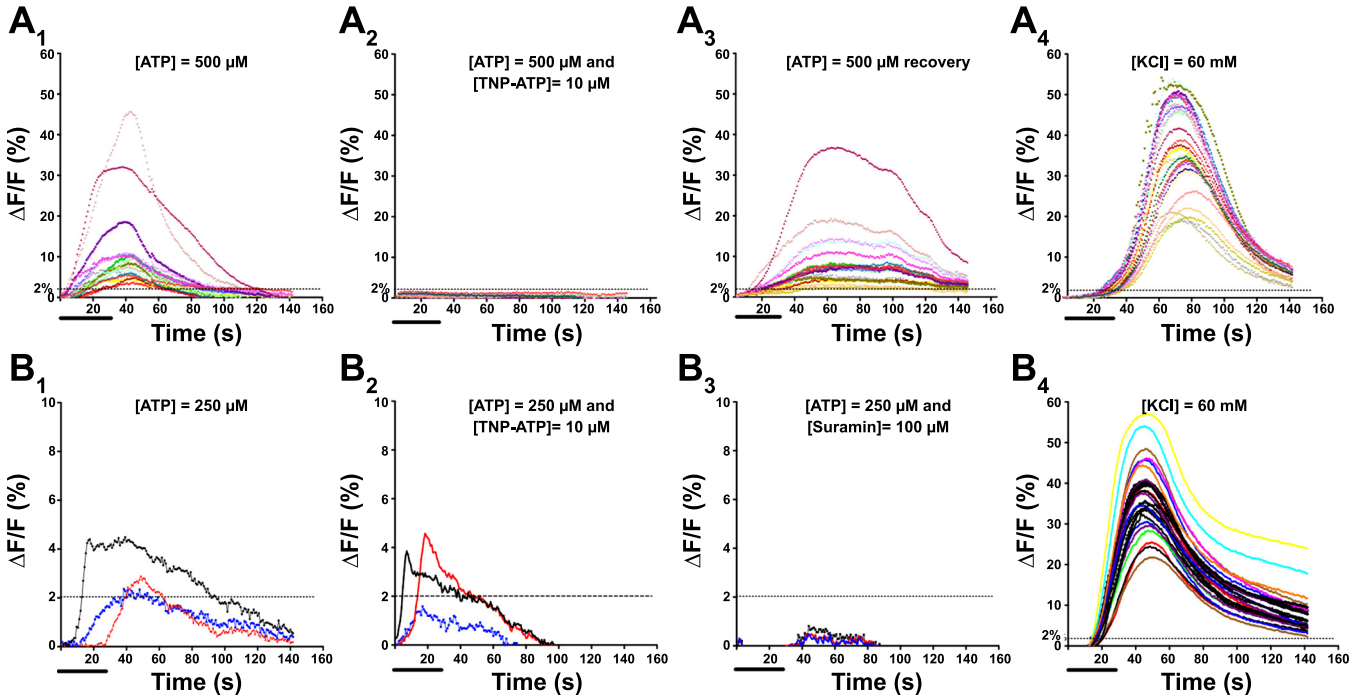

Fig. 6. Representative waveforms of PGN [Ca^{2+}]$_i$ responses to ATP in the presence or absence of TNP-ATP, a specific $P2X_1/P2X_3/P2X_{2/3}$ antagonist, or suramin, a nonselective P2 purinergic receptor antagonist. Percent change in mean fluorescence intensity (ΔF%) reflecting [Ca^{2+}]$_i$ response in PGN from P5–8 animals (A_1–A_4) or P19–25 animals (B_1–B_4). In preparations from P5–8 animals, [Ca^{2+}]$_i$ responses to 500 μM ATP (R2 type, A_1), were blocked completely by TNP-ATP (10 μM, A_2) and recovered 30 min after washout (A_3). In P19–25 animals, ATP (250 μM) induced [Ca^{2+}]$_i$ responses R3 and R2 (B_1), which were not blocked completely by TNP-ATP (10 μM, B_2), but were blocked nearly completely by suramin (100 μM, B_3). Cells were exposed to ATP for 30 s (bar). Viability of PGNs was demonstrated at the end of each experiment by their brisk response to KCl (60 mM) (A_4 and B_4).

the petrosal ganglia. A slow [Ca^{2+}]$_i$-response pattern (R2) predominates in younger animals, whereas fast (R1) and intermediate (R3) [Ca^{2+}]$_i$-response patterns predominate in older animals. These differences in [Ca^{2+}]$_i$-response patterns may be related to changes in P2XR isoform expression that also change in the same postnatal period.

This study is the first to optically record [Ca^{2+}]$_i$ responses to ATP in a population of chemoafferent cell bodies in the PG. Previously we demonstrated that PG neurons similarly retrogradely labeled with rhodamine dextran-amine (RDA) express tyrosine hydroxylase and have a localization consistent with chemoafferent neurons (31), indicating that the retrograde labeling primarily targets chemoreceptor afferent neurons. Our optical recording approach uniquely allows the simultaneous evaluation of responses in multiple chemoafferent neurons at single-cell resolution. This is in contrast to electrophysiological approaches, which are limited to single neuron recording or summated multiunit population recordings (20, 22, 32, 33). Differences in species, age, and methodology may explain the lower number of ATP-[Ca^{2+}]$_i$-responsive cells within the population of chemoafferent neurons observed in our experiments compared with reports using patch-clamped PGN from adult cat (33).

The results presented here are in agreement with previous reports highlighting the role of P2XR in initiating chemoafferent activity in rodents. ATP activates $P2X_2$ and $P2X_3$ receptors postsynaptically (37). $P2X_2$ and $P2X_3$ protein is present in afferent fibers within the carotid body and mRNA is present in the PG neuronal soma (22, 25, 37). The deletion of genes encoding $P2X_2$ and $P2X_3$ causes a reduction in the afferent nerve response to hypoxia (25). Although the contribution of ATP acting through P2 receptors is established in rodents, its role in hypoxia-mediated chemoexcitation is still uncertain in other species as demonstrated by the contradictory effects on hypoxia stimulated chemodischarge observed in cats following inhibition of P2 receptors (24, 33).

The role of purinergic receptors in chemosensitivity during development has not been well explored. Chemoreceptors are immature at birth and there is evidence for a relatively low initial sensitivity to hypoxia with maturation to adult levels occurring over the first 2–3 wk of life. Part of this maturation is due to biophysical changes in the properties of glomus cells (36). These cells respond to hypoxia with a depolarization and influx of calcium through voltage-gated channels. Both the magnitude of depolarization and the magnitude of hypoxia-induced calcium changes increase during the postnatal period (28, 35). In addition, hypoxia-induced catecholamine release increases during the postnatal period (6). At present it is unknown whether this is also true for ATP release, but this seems likely given that catecholamine storage vesicles contain high concentrations of ATP (30). If there is a fixed linear relationship between ATP and catecholamine release within the carotid body in response to hypoxia, then ATP release should also increase with development. Although real-time release of ATP from the carotid body in response to hypoxia has been reported (4, 17), its developmental profile has not. This is the first report to describe the calcium response profile induced by exogenous ATP of petrosal chemoreceptor neurons and its change over postnatal development. The present experiments were not designed to test the response profiles at the

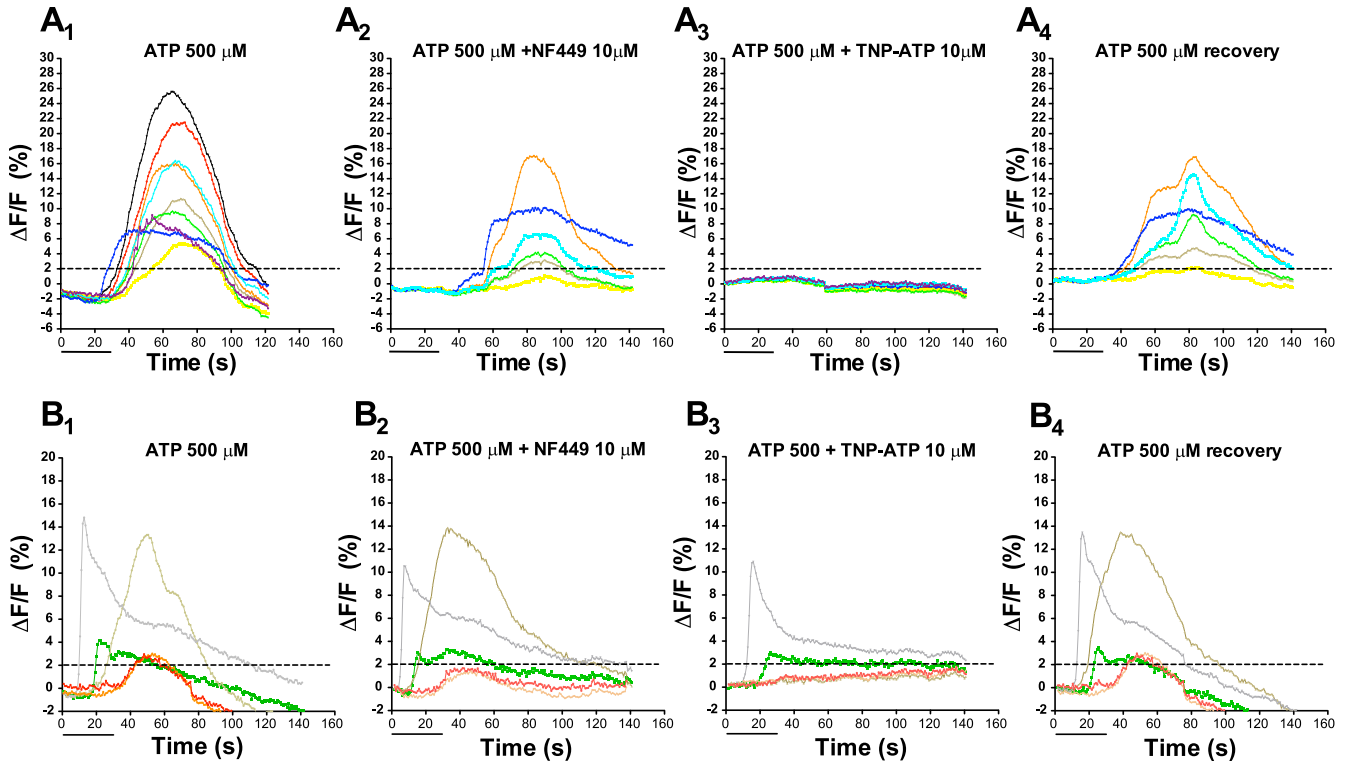

Fig. 7. Representative $[Ca^{2+}]_i$ responses to ATP in the presence or absence of TNP-ATP (10 μM) or the selective $P2X_1$ receptor antagonist NF449 (10 μM) in PGNs from P5–8 (A_1–A_4) or P19–25 animals (B_1–B_4). NF449 had only a slight effect on responses (A_2, B_2), whereas TNP-ATP markedly inhibited $[Ca^{2+}]_i$ responses (A_3, B_3), especially in the younger animals (A_3).

afferent nerve terminals or the profile of response to endogenous ATP release.

We observed that the average response magnitudes of chemosensory afferents in the PG seen with increasing concentrations of ATP were not different between the older and younger age groups (Fig. 3). This is consistent with the finding that antagonism of purinergic transmission with suramin or A317491 (a $P2X_3$ receptor blocker) reduces the ventilatory response to hypoxia and chemoreceptor activity in equal degree across early development (18).

In contrast to the magnitude of response the temporal response patterns (rise and decay of $[Ca^{2+}]_i$) changed significantly during the postnatal period. Labeled PGNs exhibited different response patterns to ATP characterized by their activation and decay times: a fast (R1), a slow (R2), and an intermediate (R3) response waveform. Similar response profiles have been previously reported in the inward currents produced by ATP application to rat trigeminal neurons (16).

The differing response profiles are likely related to different P2X isoforms. In electrophysiological experiments, ATP-sensitive cells have rapidly, slowly, or nondesensitizing responses to exogenous ATP, and these response types can be related to the P2XR subunit composition (7, 16). For instance, ATP application produces a transient current in HEK cells expressing $P2X_1$ or $P2X_3$, but a relatively sustained current in cells expressing $P2X_2$ receptors (7). In voltage-clamp experiments, $P2X_1$ and $P2X_3$ have a fast R1 pattern, $P2X_2$ and $P2X_4$ have a response pattern similar to R3, and the response of coexpressed $P2X_2$ and $P2X_3$ resembles R2 (19). In our experiments, the time courses for ATP-induced $[Ca^{2+}]_i$ signal were longer than the currents previously reported (19), which reflects the time needed for the calcium to be eliminated from the cytoplasm by several mechanisms. Additionally, the presence of P2X heteromer receptors can increase the time course of the response: fast P2X1 receptors could be expressed as P2X1/5 mediating

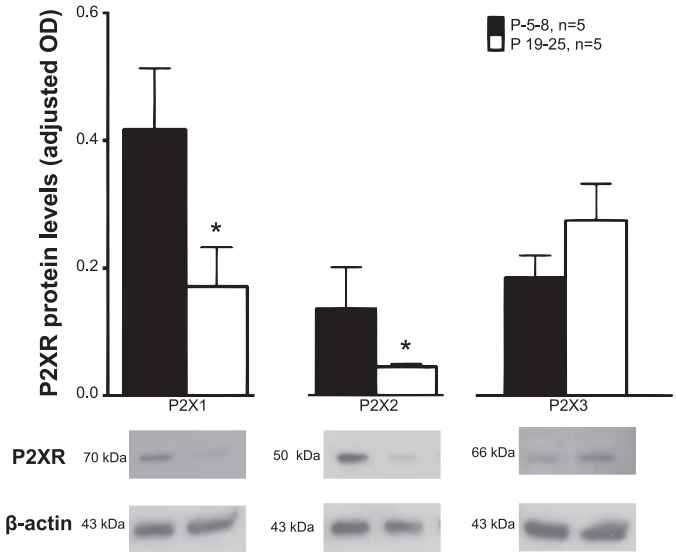

Fig. 8. Western blot showing changes in P2X receptor (P2XR) profile in homogenates of the petrosal ganglia (PG) from P5–8 and P19–25 animals. Representative bands corresponding to the molecular weight of the P2X receptor subtype $P2X_1$, $P2X_2$, and $P2X_3$ along with β-actin as an internal loading control. $^*P < 0.05$, unpaired *t*-test; *n,* number of litters.

slower response. The slow R2 is the predominant pattern observed in younger animals, and it is virtually eliminated by TNP-ATP, a $P2X_1$, $P2X_3$, and $P2X_{2/3}$ antagonist (34) and a likely $P2X_{1/5}$ inhibitor (11, 29). R1 and R3 were observed in older animals and were partially blocked by TNP-ATP. A contribution of the $P2X_1$ receptor to the $[Ca^{2+}]_i$ responses of PGNs to ATP was seen at both development ages. By expanding the receptor blockade using suramin, a nonselective P2 purinergic receptor antagonist that inhibits P2Y, $P2X_1$, $P2X_2$, $P2X_3$, $P2X_5$, and $P2X_7$ (23), complete blockade was observed, suggesting that additional P2XR isoforms contribute to the ATP response of PGNs with maturation. It should also be noted that response profiles do not translate across species since the response to exogenous ATP appears to be different in the cat (33) than we have observed in the rat.

The developmental P2X isoform expression profile is consistent with the changes seen in pharmacological sensitivity. Both $P2X_1$ and $P2X_2$ protein levels decrease in the PG with postnatal development, a finding consistent with the developmental decrease in $P2X_2$ protein levels observed in the PG of the cat (2). A slight developmental decrease in $P2X_3$ protein levels has also been reported in the PG of the cat (2), but we found no significant change in $P2X_3$ protein levels in the rat. Thus developmental changes in the expression of different isoforms may differ among species. The changing expression profile of $P2X_1$ and $P2X_2$ with maturation in the rat PG could account for the observation that the combined $P2X_1$, $P2X_3$, and $P2X_{2/3}$ blocker (TNP-ATP) affects the ATP-response profile of PGNs differently during postnatal development.

The significance of the change in the $[Ca^{2+}]_i$ response profiles to ATP in peripheral arterial chemoreceptors is not known. However, in other organ systems fast ATP-induced $[Ca^{2+}]_i$ responses underlay impulse activity whereas slow ATP-induced $[Ca^{2+}]_i$ responses mediate plasticity, as described in skeletal muscle (5). It is therefore tempting to speculate that the slow R2 response that is prominent during early postnatal life may be an indication of plastic changes in synaptic traffic within the carotid body chemosensory system.

The interpretation of our data is limited by several factors that deserve discussion. First, bath application of ATP may lead to concentrations higher than endogenous ATP concentrations at the synapse, although it is estimated that the concentration of some transmitters in the synaptic cleft is >0.5 mM (i.e. acetylcholine at the neuromuscular junction; 27). The ATP bath concentrations that we used are similar to those used in organotypic cultures of brain slices and in preparations containing carotid body attached to the sinus nerve (14, 25). We titrated the concentration of ATP until a response was observed. In preliminary experiments PGNs did not respond at concentrations lower than 250 μM (data not shown). Second, we measured $[Ca^{2+}]_i$ responses in the PGN somata, which could be caused by direct activation of somal P2XRs or by voltage-gated calcium channels activated by postsynaptic action potentials, in addition to activation of synaptic P2XRs. Thus we cannot define the specific contribution of synaptic P2XRs to the overall calcium response. Third, we used protein homogenates of the whole petrosal ganglia for Western blot, and thus assayed protein expression in chemosensitive and nonchemosensitive neuron populations simultaneously. Fourth, it is likely that cell bodies of both chemoreceptors and baroreceptors were labeled when the dye was applied to the cut carotid sinus nerve. When the dye was applied to the carotid body, only cell bodies of chemoreceptors should be labeled, and the responses were similar with both labeling techniques. Nevertheless, it is possible that combined analysis may include a small number of cell bodies from baroreceptors. Moreover, we counted the number of labeled chemosensitive neurons only in the distal portion of the petrosal ganglion and thus may have missed chemosensitive neurons located in other regions of the nodose/petrosal complex. Also, since our experiments were done in single cells within the tissue, changes in calcium from cells underneath the region of interest and fibers in passage may contribute to the slow time courses of ATP-induced $[Ca^{2+}]_i$ responses. Nevertheless, our Western blot data are consistent with the pharmacological data showing that $P2X_1$, $P2X_3$, and $P2X_{2/3}$ receptors contribute to mediating the $[Ca^{2+}]_i$ responses to ATP in the chemoafferents. Last, these experiments were not powered to determine sex differences.

Our pharmacological approach adds to the literature by demonstrating that $P2X_1$ receptors participate in the response of PGNs to ATP in young and older animals, and that P2X receptors other than P2X1, P2X3, and P2X2/3 have a major role in mediating the ATP response in older animals. Although other studies conclude that $P2X_2$ and $P2X_3$ isoforms are primarily responsible for hypoxic chemosensitivity (22, 25), the carotid body is also responsive to other blood borne factors such as glucose and cytokines (15, 21). It is not known whether the P2XRs that are responsive to ATP on chemoafferents are also involved in mediating carotid body responses to stimuli other than hypoxia.

In summary, using optical recording in an ex vivo preparation of retrogradely labeled chemoafferents, we demonstrate a developmental change in $[Ca^{2+}]_i$ responses to ATP in PGNs that is correlated with a change in the relative expression of different P2XR isoforms. Our data suggest that changes in P2XR isoform expression play an important role in mediating the postnatal increase in chemoreceptor responsiveness to hypoxia and other stimuli.

GRANTS

This work was financially supported by National Heart, Lung, and Blood Institute Grant R01-HL-072748 (E. B. Gauda) and by the Science and Technology Foundation Fellowship (SFRH/BD/ 39473/2007, A. R. Nunes).

DISCLOSURES

No conflicts of interest, financial or otherwise, are declared by the author(s).

AUTHOR CONTRIBUTIONS

Author contributions: A.R.N. and E.B.G. conception and design of research; A.R.N., T.E., and E.B.G. performed experiments; A.R.N. and R.C.-V. analyzed data; A.R.N., R.C.-V., D.F.D., J.C.G., and E.B.G. interpreted results of experiments; A.R.N. prepared figures; A.R.N. and E.B.G. drafted manuscript; A.R.N., R.C.-V., T.E., D.F.D., J.C.G., and E.B.G. edited and revised manuscript; A.R.N., R.C.-V., T.E., D.F.D., J.C.G., and E.B.G. approved final version of manuscript.

REFERENCES

1. **Alcayaga C, Varas R, Valdés V, Cerpa V, Arroyo J, Iturriaga R, Alcayaga J.** ATP- and ACh-induced responses in isolated cat petrosal ganglion neurons. *Brain Res* 1131: 60–67, 2007.
2. **Bairam A, Joseph V, Lajeunesse Y, Kinkead R.** Developmental profile of cholinergic and purinergic traits and receptors in peripheral chemoreflex pathway in cats. *Neuroscience* 146: 1841–1853, 2007.

3. **Bradford MM.** A rapid and sensitive method for the quantitation of microgram quantities of protein utilizing the principle of protein-dye binding. *Anal Biochem* 72: 248–254, 1976.
4. **Buttigieg J, Nurse CA.** Detection of hypoxia-evoked ATP release from chemoreceptor cells of the rat carotid body. *Biochem Biophys Res Commun* 322: 82–87, 2004.
5. **Buvinic S, Almarza G, Bustamante M, Casas M, Lopez J, Riquelme M, Saez JC, Huidobro-Toro JP, Jaimovich E.** ATP released by electrical stimuli elicits calcium transients and gene expression in skeletal muscle. *J Biol Chem* 284: 34490–34505, 2009.
6. **Donnelly DF, Doyle TP.** Developmental changes in hypoxia-induced catecholamine release from rat carotid body, in vitro. *J Physiol* 475: 267–275, 1994.
7. **Egan TM, Samways DS, Li Z.** Biophysics of P2X receptors. *Pflügers Arch* 452: 501–512, 2006.
8. **Finley JC, Polak J, Katz DM.** Transmitter diversity in carotid body afferent neurons: dopaminergic and peptidergic phenotypes. *Neuroscience* 51: 973–987, 1992.
9. **Glover JC.** Retrograde and anterograde axonal tracing with fluorescent dextrans in the embryonic nervous system. *Neurosci Protocols* 30: 1–13, 1995.
10. **Gonzalez C, Almaraz L, Obeso A, Rigual R.** Carotid body chemoreceptors: from natural stimuli to sensory discharges. *Physiol Rev* 74: 829–898, 1994.
11. **Haines WR, Torres GE, Voigt MM, Egan TM.** Properties of the novel ATP-gated ionotropic receptor composed of the P2X(1) and P2X(5) isoforms. *Mol Pharmacol* 56: 720–727, 1999.
12. **Katz DM, Black IB.** Expression and regulation of catecholaminergic traits in primary sensory neurons: relationship to target innervation in vivo. *J Neurosci* 6: 983–989, 1986.
13. **Kholwadwala D, Donnelly DF.** Maturation of carotid chemoreceptor sensitivity to hypoxia: in vitro studies in the newborn rat. *J Physiol* 453: 461–473, 1992.
14. **Lalo U, Voitenko N, Kostyuk P.** Iono- and metabotropically induced purinergic calcium signaling in rat neocortical neurons. *Brain Res* 799: 285–291, 1998.
15. **Liu X, He L, Stensaas L, Dinger B, Fidone S.** Adaptation to chronic hypoxia involves immune cell invasion and increased expression of inflammatory cytokines in rat carotid body. *Am J Physiol Lung Cell Mol Physiol* 296: L158–L166, 2009.
16. **Luo J, Yin GF, Gu YZ, Liu Y, Dai JP, Li C, Li ZW.** Characterization of three types of ATP-activated current in relation to P2X subunits in rat trigeminal ganglion neurons. *Brain Res* 1115: 9–15, 2006.
17. **Masson JF, Kranz C, Mizaikoff B, Gauda EB.** Amperometric ATP microbiosensors for the analysis of chemosensitivity at rat carotid bodies. *Anal Chem* 80: 3991–3998, 2008.
18. **Niane LM, Donnelly DF, Joseph V, Bairam A.** Ventilatory and carotid body chemoreceptor responses to purinergic P2X receptor antagonists in newborn rats. *J Appl Physiol* 110: 83–94, 2011.
19. **North RA.** Molecular physiology of P2X receptors. *Physiol Rev* 82: 1013–1067, 2002.
20. **Nurse CA, Zhang M.** Acetylcholine contributes to hypoxic chemotransmission in co-cultures of rat type 1 cells and petrosal neurons. *Respir Physiol* 115: 189–199, 1999.
21. **Pardal R, Lopez-Barneo J.** Low glucose-sensing cells in the carotid body. *Nat Neurosci* 5: 197–198, 2002.
22. **Prasad M, Fearon IM, Zhang M, Laing M, Vollmer C, Nurse CA.** Expression of P2X2 and P2X3 receptor subunits in rat carotid body afferent neurons: role in chemosensory signaling. *J Physiol* 537: 667–677, 2001.
23. **Ralevic V, Burnstock G.** Receptors for purines and pyrimidines. *Pharmacol Rev* 50: 413–492, 1998.
24. **Reyes EP, Fernandez R, Larrain C, Zapata P.** Carotid body chemosensory activity and ventilatory chemoreflexes in cats persist after combined cholinergic-purinergic block. *Respir Physiol Neurobiol* 156: 23–32, 2007.
25. **Rong W, Gourine AV, Cockayne DA, Xiang Z, Ford AP, Spyer KM, Burnstock G.** Pivotal role of nucleotide P2X2 receptor subunit of the ATP-gated ion channel mediating ventilatory responses to hypoxia. *J Neurosci* 23: 11315–11321, 2003.
26. **Sitsapesan R, Williams AJ.** Modification of the conductance and gating properties of ryanodine receptors by suramin. *J Membr Biol* 153: 93–103, 1996.
27. **Slater CR.** Reliability of neuromuscular transmission and how it is maintained. *Handb Clin Neurol* 91: 27–101, 2008.
28. **Sterni LM, Bamford OS, Tomares SM, Montrose MH, Carroll JL.** Developmental changes in intracellular Ca^{2+} response of carotid chemoreceptor cells to hypoxia. *Am J Physiol Lung Cell Mol Physiol* 268: L801–L808, 1995.
29. **Surprenant A, Schneider DA, Wilson HL, Galligan JJ, North RA.** Functional properties of heteromeric P2X(1/5) receptors expressed in HEK cells and excitatory junction potentials in guinea-pig submucosal arterioles. *J Auton Nerv Syst* 81: 249–263, 2000.
30. **Taupenot L, Harper KL, O'Connor DT.** The chromogranin-secretogranin family. *N Engl J Med* 348: 1134–1149, 2003.
31. **Tolosa JN, Cooper R, Myers AC, McLemore GL, Northington F, Gauda EB.** Ontogeny of retrograde labeled chemoafferent neurons in the newborn rat nodose-petrosal ganglion complex: an ex vivo preparation. *Neurosci Lett* 384: 48–53, 2005.
32. **Varas R, Alcayaga J, Zapata P.** Acetylcholine sensitivity in sensory neurons dissociated from the cat petrosal ganglion. *Brain Res* 882: 201–205, 2000.
33. **Varas R, Alcayaga J, Iturriaga R.** ACh and ATP mediate excitatory transmission in cat carotid identified chemoreceptor units in vitro. *Brain Res* 988: 154–163, 2003.
34. **Virginio C, Robertson G, Surprenant A, North RA.** Trinitrophenyl-substituted nucleotides are potent antagonists selective for P2X1, P2X3 and heteromeric P2X2/3 receptors. *Mol Pharmacol* 53: 969–973, 1998.
35. **Wasicko MJ, Sterni LM, Bamford OS, Montrose MH, Carroll JL.** Resetting and postnatal maturation of oxygen chemosensitivity in rat carotid chemoreceptor cells. *J Physiol* 514: 493–503, 1999.
36. **Wasicko MJ, Breitwieser GE, Kim I, Carroll JL.** Postnatal development of carotid body glomus cell response to hypoxia. *Respir Physiol Neurobiol* 154: 356–371, 2006.
37. **Zhang M, Zhong H, Vollmer C, Nurse CA.** Co-release of ATP and ACh mediates hypoxic signalling at rat carotid body chemoreceptors. *J Physiol* 525: 143–158, 2000.